Advances in Science and Technology Research Journal

Volume 14, Issue 2, June 2020, pages 215–222
https://doi.org/10.12913/22998624/118103

Received: 2019.01.13
Revised: 2020.03.30
Accepted: 2020.04.20
Available online: 2020.05.05

Visual Effects of Surface Emissivity in Thermal Imaging

Arkadiusz Urzędowski[1*], Dorota Wójcicka-Migasiuk[1], Barbara Buraczyńska[1]

[1] Lublin University of Technology, Fundamentals of Technology Faculty, ul. Nadbystrzycka 38, 20-618 Lublin, Poland

* Corresponding author's e-mail: a.urzedowski@pollub.pl

ABSTRACT

The article discusses the impact of surface emissivity on the thermograms, obtained from a thermal imaging camera during the measurements of construction objects. The study was carried out as an analysis of the digital and thermal images for three selected materials types of building finishing such as: wood outside doors, cement-lime plaster and glass façade. The images obtained from the exterior and from the interior of the buildings were compared and analyzed in terms of the spectrum intensity within the range of ambient temperature. The result of the conducted research shows how important it is to use both side images for such details as locks, door knobs and handles to properly assess the optional light reflections, especially on glossy surfaces. The influence of the most significant factors on the surface emissivity, such as direction of emission θ, surface temperature T_s, radiation wavelength λ, time τ, was discussed on the basis of the experiment. The measurements were made using a Flir T440bx thermal imaging camera, while for the analysis of thermal images and the generation of graphs, the Flir Tools+ 6.4.18039.1003 software was used. For all tested materials, the emissivity value was estimated using a camera and black insulating tape characterized by a known emissivity value $\varepsilon = 0.98$. The study of materials with different emissivity under the reference conditions helped to identify the influence of material reflectivity on the obtained temperature spectrum values and to correctly perform the research. The temperature ranged between 269–293 K, but in particular measurements, the range was reduced. The thermal images reveals additional unexpected details of insulation discontinuity, the indication of which is necessary for building modernization. The wood door joinery research showed the leakage, which disqualifies them from use in low energy buildings in much more definite way because the temperature range resulting from heat outflow approaches even 15 K. The use of glass wind insulation boards can eliminate the wood door icing, which occurs at a temperature of about 268 K, and at the same time, increase the temperature of the shielded door by about 10 K.

Keywords: surface emissivity, thermal imaging, building structural materials

INTRODUCTION

The thermo-visual measurements require adaptation to the special conditions occurring on the measured surface. These conditions are described by various parameters and when thermo-visual cameras are used, the most important ones are environment temperature and surface emissivity. Technical thermal evaluations are extremely important in civil engineering and building constructions oriented at low energy use. The thermal characteristics of building structural elements are required to locate and estimate the thermal bridges occurring in the construction which is supposed to be energy efficient. The presented discussion of the problem uses thermo-visual images and the images of fusion between thermal and digital pictures supported by the background of digital images of investigated elements [8, 9].

The thermal bridges can increase the risk of condensation on internal surfaces and even cause the interstitial condensation within walls and other building elements. The interstitial condensation can be exceptionally dangerous, as it cannot be seen from either the interior or exterior of the building. Condensation forms when the interior temperature drops well below the dew point and the moisture in warm air condenses into water

droplets on cooler surfaces. One of the main effects of condensation is the mould growth. Initially invisible, mould can grow out of control, causing the indoor air quality problems and negative health impacts for building occupants and then form a visible growth.

Thermal imaging measurements are one of the main non-invasive methods used for as-built inspection of building objects. However, the work on the implementation of innovative non-invasive methods for early detection and identification of fungal contamination of building materials using an e-nose is progressing. The results show that the gas sensors array consisting of MOS-type sensors enables the detection of the differences among the examined samples of fungi and distinguishing between the non-contaminated and contaminated samples [11]. Additionally, a non-invasive method of plant bioindication, focused on the improving the state of the environment in terms of the level of air pollution, has also been developed. The four indicators used to assess air quality are as follows: the degree of nitrogen air pollution, the concentration of nitrogen oxides in the air, the level of purity and the water deficit which accompanies urbanization [2, 17].

In parallel with the development of research methods, the the investigations aimed at discovering modern and environmentally friendly methods of producing building materials are being conducted. One of them is the application of flax/hemp wastes as a filling material of the lime-based composites. The composite exhibits low thermal conductivity and meets the requirements established for low-energy buildings [4]. In passive buildings, which are air tight and have high levels of insulation, the thermal bridges may have more of a detrimental effect. In fact, the thermal bridges can be responsible for a heat loss of up to 30 percent. When high levels of air tightness and insulation are required, the thermal bridges eliminate the positive effects that these properly insulated products have on a building.

MATERIALS AND METHODS

Surface emissivity factor is the parameter, which has the greatest impact on the temperature values recorded in the form of color spectrum by a thermal imaging camera. The value of this factor should be entered by the operator before the test is started. Surface emissivity is the ratio of the surface radiation intensity to perfectly the black body radiation measured at the same temperature. The values define the fraction which varies between 0 and 1, but do not reach boundary extremes. The emissivity ε as a physical phenomenon depends on many parameters, such as: direction of emission θ, surface temperature T_S, radiation wavelength λ, time τ, physical state of the surface, chemical composition, body type. These complex dependencies can be written in a general form as the function of the following variables: $\varepsilon = f(\lambda, T_S, \tau, \theta)$.

Due to the direction of wave propagation, the emissivity can be divided into: normal (direction perpendicular to the surface), directional (selected radiation direction) and semi-spherical (refers to radiation from a flat surface to the hemisphere). Due to the wavelength function, the emissivity is divided into monochromatic (for the selected wavelength of radiation) or panchromatic (for the entire radiation spectrum). In building partitions, the occurring radiative heat exchange with the external environment takes place in two ways:

- Spectral emissivity:

$$\varepsilon_\lambda = \frac{W_\lambda}{W_{b\lambda}}, \tag{1}$$

where: W_λ – monochromatic radiation intensity of a given wavelength,
$W_{b\lambda}$ – monochromatic radiation intensity of the same wavelength for a black body.

- Total emissivity:

$$\varepsilon = \frac{W_T}{W_{bT}}, \tag{2}$$

where: W_T – radiation intensity in full range for a given body,
W_{bT} – radiation intensity in full range for a black body.

The emissivity values are collected in tables, showing that such forms as ice, snow and water which occur in the ambience, are of high emissivity 0.95–0.98 (expressed as the percentage of total emissivity), but typical building materials have emissivity in range 0.80–0.95, which means that only 5 to 20% of heat radiation is reflected out off this surface. Particular attention should, however, be paid when the materials of emissivity below 0.6, such as metals or, for example, polished façade finishes, are tested, because the camera lens receives a large amount of reflected thermal radiation then. In the case where nontransparent building materials are tested, some simplifying assumptions can be applied.

Firstly, the surfaces of building construction exposed to temperature measurements can be treated as grey because they absorb some fraction of radiation independently of its wavelength. That is why ,emissivity is always important to the results in the thermal visual measurements but at the assumed range can be treated as constant. The range of the described measurements (263–293 K) is included in the middle of commonly established range for building envelope surfaces (i.e.: 243–353 K) [6, 7, 10].

Secondly, the thermal diffusion from building material surfaces forms the basis on which the thermal visual methods are useful to determine damages, thermal bridges or just improper insulation elements. This phenomenon enables us to register how the heat transfers out off particular building elements as such or when they are subjected mechanical wear or humidity increase.

The emissivity values can be assumed from the reference tables, bearing in mind that the adoption of these coefficients corresponds to the current conditions with some deviations, thus the camera operators should use their specific reference data for a specific test field [5]. This set of data will be helpful as dedicated to particular objects, specific camera models and test conditions.

MEASUREMENT RESULTS AND DISCUSSION

The thermal vision measurements were preceded by thermal imaging camera tests to determine the actual emissivity of the currently tested surfaces. A Flir T440bx camera model was used for capturing particular images. For each of the discussed pictures, emissivity was determined in an experimental way.

The study consists in determining the reflected temperature and emissivity of the tested surface as described for Figure 1. It shows an example of the test procedure repeated by the authors for particular surface emissivity under the outdoor conditions using a thermographic method. For this purpose, a fragment area of the tested object with a homogeneous surface and temperature higher than the ambient temperature was selected to obtain a high thermal contrast. On the façade of the building covered with cement-lime plaster, a black matte insulation tape was glued. Such tapes are characterized by a very high emissivity coefficient factor of 0.98 (Fig. 1-1). After one hour delay, the temperature of the tape was equalized and the same as the surface of the tested objects, the tests were started. All measurement parameters were set in the camera: relative humidity (RH = 86%), distance between the object and the camera (l = 2.0 m), object emissivity (0.98), atmosphere temperature (T = 270.15 K), its middle measuring point was directed at the insulating tape and temperature readouts showed 0.1°C (Fig. 1-2). The subsequent measurements were carried out for a fragment of the surface outside the tape and reached -0.6°C (Fig. 1-3). In further steps of camera settings, the operator repeatedly changed the emissivity values and recorded the results until the point readings of temperature values equalized (Fig. 1-4). When receiving the same temperature values from the tape and from the surface of the tested object, the entered emissivity value was 0.87 and it was established as sufficiently good approximation of the emissivity for the current test surface.

The presented case measurements performed by means of a digital thermal-visual FLIR T440bx camera enabled to understand the interference of surface emissivity in thermal measurements. They represent only the selected cases from the authors' data base. The used camera also enables to measure the difficult to reach surfaces, but at the same time the measurement results are vulnerable to physical parameters (emissivity in particular) and the reference temperature. In the case where the energy emission is caused additionally by the surface reflectance, the percentage of reflections balance the temperature influence and can be estimated at such percentage proportion without the risk of misrepresentation for the building measurement applications. The perfect measurement laboratory conditions are usually hardly available during in site measurements in natural urban environment [1, 3, 4].

The presented row of images shows the same window located on the north-west oriented building element in a shadowed area. This orientation enables to avoid the direct sun radiation reflections, but the reflected radiation beam is still visible. This has an immediate influence on the thermal measurement indications, making them less clear. In such cases the reliability of measurements can be supported by careful interpretation in Figure 2.

Figure 2-1 presents the digital photo of a segment window oriented and shadowed from the direct beam. The visible buildings are reflected in glasses and show illuminated walls. Figure 2-2 shows the image called fusion between the

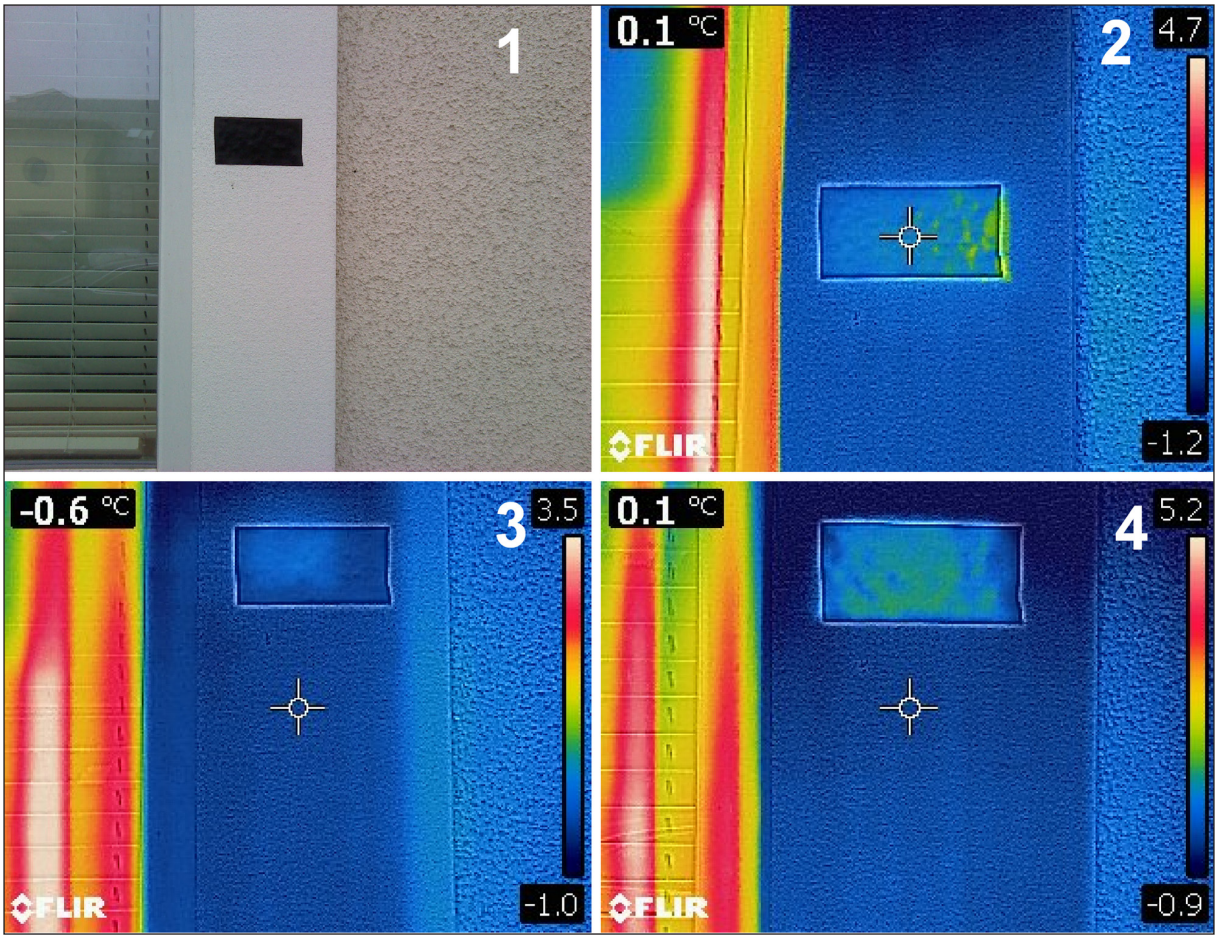

Fig. 1. Determination of surface emissivity using a thermal imaging camera

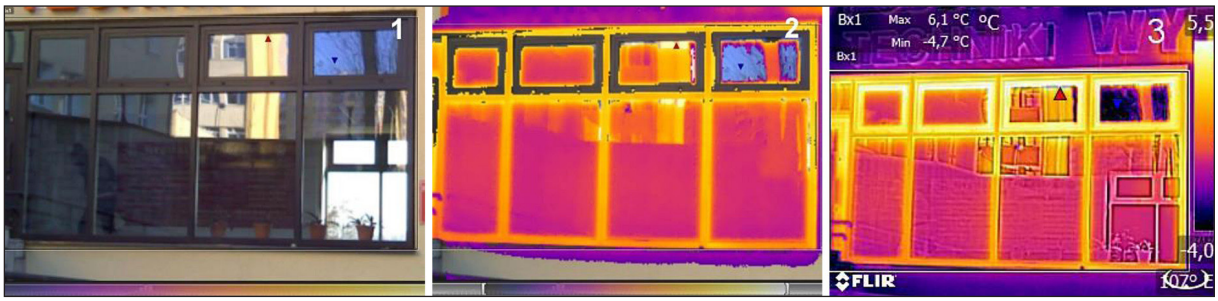

Fig. 2. The set of images from thermal-visual camera of the same façade element (1 – digital photo, 2 – fusion image, 3 – thermal image)

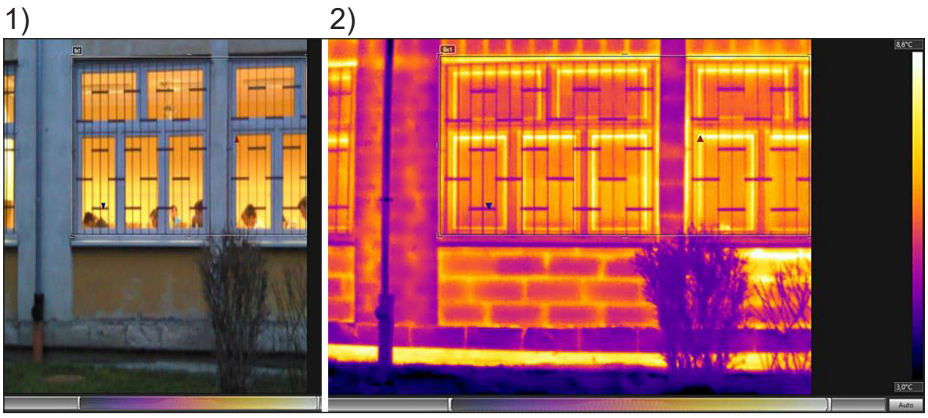

Fig. 3. The comparison of digital (1) and thermal (2) images subjected to interpretation

a)

thermal and digital pictures. The digital picture defunct at higher emissivity under the colorful interpretation of the registered values regardless if the reflectance comes from light or from temperature measurements. The window frame is not reflective, thus no colour (or visible grayscale) is allocated to allow reliable temperature readouts (Fig. 2-3). The complete thermal image shows the obvious thermal bridges in the places of window frames where windows have opening elements. Thus, their seals are not sufficiently tight. The temperature difference between the properly insulated wall area and the heat leaking frames is about 6 K, while the difference between fixed stiff elements is about 2 K, which is not recognized as a thermal bridge. Large glass panels of high reflectance still show the reflected images of the surroundings. This particular option of visualization is the MSX module, in which the thermal image is presented with the background of the digital one [2].

Another case is presented in Figure 3-1 and 3-2, where perfect emissivity test conditions occur and are indicated to perform the thermal–visual measurements by means of the same camera as previously described. This image shows a building element supposed to undergo complex modernization and refurbishment. The observed damage to the bottom plaster band matches its very low thermal insulating properties. The image reveals the very low quality of the walls under the windows and the bottom band, through which the thermal flux leaks with the temperature difference of 5 K. At such moderate ambient temperature as 3.5 K, the thermal bridge appears to be substantial [1, 11, 13]. The readouts are possible in Figure 3-2. The thermal image reveals additional unexpected details. The bottom band of the visible low quality plaster performs quite well thermally but the most intensive leakage occurs below. This is the indication for the necessary modernization of this building foundation, which would definitely need such reliable justification for digging out the foundation and installing new insulation. Unexpectedly, the vertical pillars perform well, allowing only 1 K temperature difference.

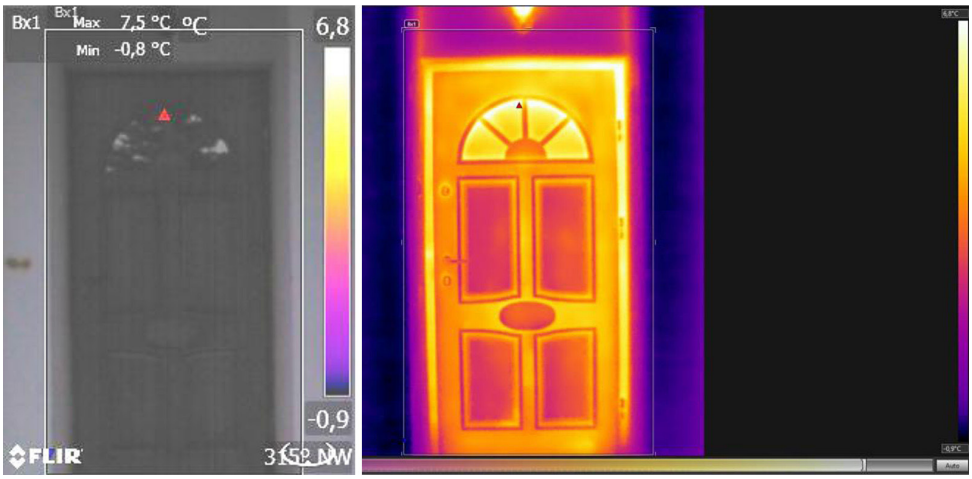

Fig. 4. Common design standard door in housing estates

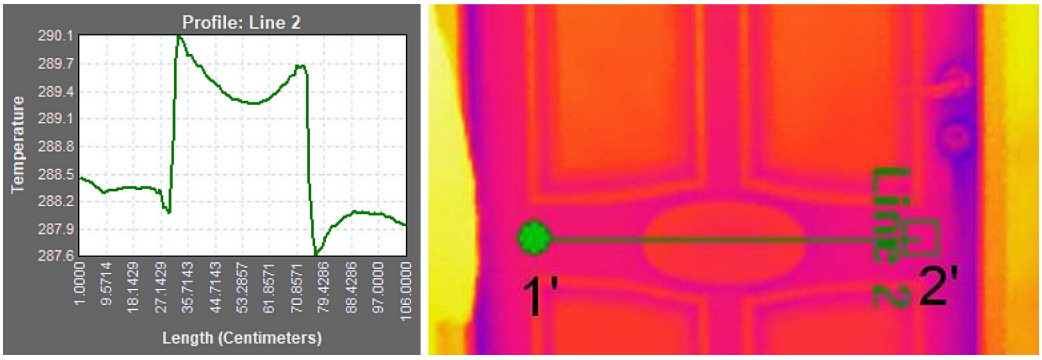

Fig. 5. Temperature waveform along horizontal axis presented in inside view

Figure 4 presents a standard door of supposed good quality in marketing. The frame is metal and the first impression tells of uneven orifice mounting. The second glance indicates the proper thickness as a door should have and that the daylight inlet should be organized in another way, which could be tighter for the heat flux. Assuming mild ambient conditions at 272.1 K and the temperature difference of 8 K, one can expect frost on the front threshold inside a house at 263 K outside temperature, which is quite common in the winter season. While convex glass gives reflections and could provide unreliable measurement results, the most important edges are characterized by emissivity of 95%. Nevertheless, it is important to use both side images for such details as locks, door knobs and handles to assess properly optional light reflections on glossy surfaces. Figure 4 presents a thermal image which reveals uneven front planes of the frame, the door wing and even its filling and also the consequence of a common installation method without the thermal flux control. The adjacent temperature scale is the same in both photos.

The evaluation of the objects presented in visual form in Figures 2-4 can be more informative, accurate and reliable when heat transfer analysis is performed too. In the presented cases, the authors used Flir Tools+ 6.4.18039.1003 software, mostly to show the distribution of the heat flux on the external surfaces and transient temperature waveform in selected areas. The presented waveform (Fig. 5) shows the temperature range within 2.5 K which is unexpectedly high on the surface that is supposed to form an evenly applied insulated element to prevent the heat outflow. Visible decoration elements form an additional insulation, but this is insufficient and should rather be replaced with an additional protective layer.

The visible heat outflow around the door surface is not related to the door surface construction but to improper frame holdfast leak, including the keyhole and door handle. This leakage disqualifies the use of this door from low energy buildings, in much more definite way, because the temperature range resulting from the heat outflow approaches even 15 K, under comparatively mild winter ambient conditions (269 K) taking into account that the computational ambient temperature for the envelope is 253 K in this climatic zone. The conditions actually measured allow frost to form in the frame, which directly leads to the subsequent deformations in the frame and greater frost accumulation in the result. This, in turn, leads to the conclusion that the frame and the closing mechanism should be much tighter. This can be achieved by the use of hinges, tightening band and two locks assuming the frame is dedicated to particular door, similarly as in the tight window frames. An additional barrier preventing from the ice and snow formation in the threshold area is necessary then to avoid deformations, which is of higher importance because of the higher cost of such quality door. Then, test can be made according to the principle rule: first protect from loss then efficiency. Additional analysis of the exterior image can bring some details to the considerations (Fig. 6). The seemingly uniform surfaces around the decoration and in the bottom part of the door plane show a non-uniform heat transfer. Unexpectedly, the material the decoration was made of, soaked up water from the melting snow on its surface at a temperature around 273 K and became more thermally conductive. This external view explains why the both graphs show mirror relation in the temperature special picks above the decorative element. Even the metal hinges form thermal bridges, especially in the bottom of this construction. They are covered within the frame and thus invisible from the interior but they are cooled together with the frame to the ambient

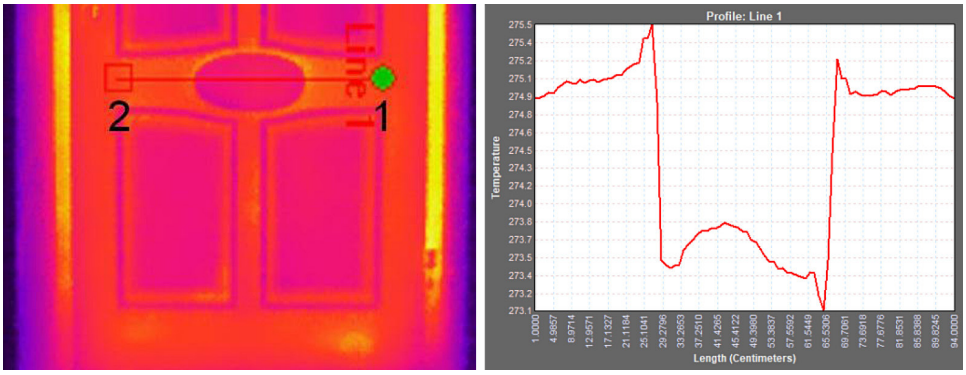

Fig. 6. Exterior image with visible additional heat leakage and its waveform

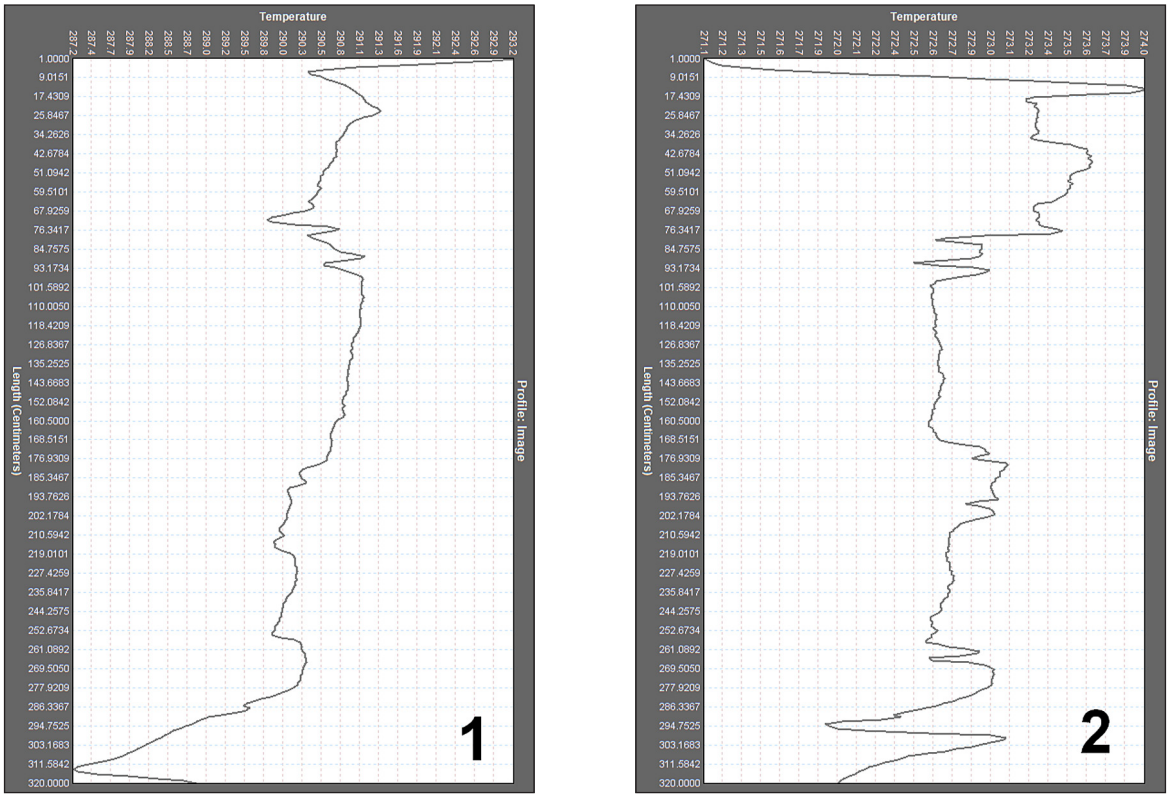

Fig. 7. Temperature waveform profile taken on the door from the interior (1) and exterior (2) in vertical position showing the dependence of the recorded temperature on the distance

temperature. Moreover, the deformations in the bottom part panel must have occurred when the users wanted to press this spot as close to the door as possible. All these results could have appeared during the first season of use [12, 14].

The consideration presented above is an additional analysis of details and can be performed for total elements such as doors or other entrance to the building space envelope as, for instance, garage gates. Figures 7 present the total element temperature waveform example but with relation to the full set of measurement points available for a particular thermo-visual tool.

Figure 7 is quite informative for the inhabitants, because it enables to imagine the amount of heat transferring through a door panel. The conditions of this measurement are comparative to the ones in detail images, i.e.: ambient temperature 271 K, interior temperature 293 K, surface emissivity 0.95. The presented mirror views on the door panel are not equally opposite because of different decoration details on both sides and the different temperature values as a result of the heat transfer. Nevertheless, it constitutes a good tool for motivating the inhabitants to start modernization towards passive housing.

CONCLUSIONS

Both side images are relevant for an appropriate interpretation of the thermo-visual images, especially when light reflections are likely to occur. The leakage through thermal bridges in passive building envelope elements is considered when 1 K drop is measured. The modernization of low energy buildings towards passive buildings require totally tight windows and door frames. The doors might require additional seasonal wind/snow fall barriers similar to balcony glass housing developments or transparent sliding shields.

The first remark is that prior to the performance of thermal imaging tests, correctly entering the emissivity value to the measuring device is the most important (among all other required parameters) because this value strongly affects the visual effect of the measurement. This value can be read out from the reference emissivity tables, but a thorough research requires determining emissivity under given environment conditions using measuring devices, including a thermal imaging camera. The authors' experience allows estimating the discrepancies in the recorded temperature, reaching the values up to 30%, depending on the

emissivity setting. Moreover, such measurement, for a selected surface, should be performed using the same thermal imaging camera that is used for the tests and with the reference surface characterized by a reliable value of high emissivity factor (as described for Figure 1).

Setting certain surface emissivity values in the thermal imaging camera results in the overstated or understated temperature values of the tested objects. The effect of emissivity on the temperature reading of selected materials (glass – theoretical emissivity of 0.95, cement-lime plaster – 0.90, wood – 0.89) at ambient temperature 296.15 K was tested. The surface emissivity values of the thermal imaging camera were changed in the sequence: 1, 0.9, 0.65, 0.3. The temperature values reached extremes for glass in the range of 0.9K, and for plaster 4.4K, for wood in the range of 4.8K. It shows that conducting measurements of the materials, the surfaces of which are characterized by high emissivity coefficients ($\varepsilon \geq 0.80$), is not always associated with a high risk of making an error, because then the reflection coefficient can be relatively small ($r \leq 0.20$). Nevertheless, the tests of reflective materials will lead to some distortion of the thermal imaging and numerous reflections; thus, such measurements should be performed from several different locations in the directions other than normal to the surface. Providing the correct emissivity value is especially important when there are large temperature differences between the tested object and environment which occur at the thermal bridges in buildings.

REFERENCES

1. Avdelidis N.P. and Moropoulou A. Emissivity considerations in building thermography. Energy and Buildings, 35(7), 2003, 663–667.
2. Babko R., Szulżyk-Cieplak J., Danko Y., Duda S., Kirichenko-Babko M., Łagód G. Effect of stormwater system on the receiver. Journal of Ecological Engineering, 20(6), 2019, 52-59.
3. Balaras C. and Argitiou A.A. Infrared thermography for building diagnostics. Energy and buildings, 34(2), 2002, 171–183.
4. Brzyski P., Barnat-Hunek D., Suchorab Z., Łagód G. Composite materials based on hemp and flax for low-energy buildings. Materials, 10(5), 2017,
5. Lo T.Y. and Choi K.T.W. Building defects diagnosis by infrared thermography. Structural Survey, 22(5), 2004, 259-263.
6. Maldague X. et al. Theory and practice of infrared technology for nondestructive testing, 2001.
7. Marynowicz A. Determination of building construction material thermal properties by means of thermal vision technique (in Polish). Oficyna Wydawnicza Politechniki Opolskiej, 165, 2019.
8. Nowak H. Application of thermal vision in civil engineering (in Polish). Oficyna Wydawnicza Politechniki Wrocławskiej, 332, 2012.
9. Rudowski G. Thermal vision and its applications (in Polish). Wydawnictwa Komunikacji i Łączności, 210, 1978.
10. Styczeń J. and Urzędowski A. Application of thermal vision measurements to determine quality of heat loss in small houses.(in Polish) [In:] Wybrane zagadnienia w zakresie budownictwa, architektury i gospodarki przestrzennej, 2017, 109–120.
11. Suchorab Z., Frac M., Guz Ł., Oszust K., Łagód G., Gryta A., Biliśka-Wielgus N., Czerwiński J. A method for early detection and identification of fungal contamination of building materials using e-nose, PLoS One, 14(4), 2019, 1-17.
12. Urzędowski A., Wójcicka-Migasiuk D. and Styczeń J. Analysis of thermal properties and heat loss in construction and isothermal materials of multilayer building walls. Advances in Science and Technology Research Journal, 11(2), 2017, 33–37.
13. Urzędowski A. and Wójcicka-Migasiuk D., Visual analysis of heat transport in unique object, Advances in Science and Technology Research Journal, 28(9), 2015, 153–159.
14. Van De Walle W. and Janssen H. Validation of a 3D pore scale prediction model for the thermal conductivity of porous building materials. 11th Nordic Symposium on Building Physics, NSB2017, 11-14 June 2017, Trondheim, Norway, Energy Procedia 132, 2017, 225–230.
15. Vollmer M. and Möllmann K.P. Infrared thermal imaging: fundamentals, research and applications. John Wiley & Sons, 2017.
16. Wójcicka-Migasiuk D. and Paśnikowska-Łukaszuk M. Rola bezpieczeństwa energetycznego w infrastrukturze budowlanej. [In:] D. Wójcicka-Migasiuk (Ed.) Wybrane aspekty bezpieczeństwa w technice i gospodarowaniu energią, Wydawnictwo Politechniki Lubelskiej, Lublin, 2019, 96–104.
17. Yoshitaka O., Hiura T., Bryophytes as bioindicators of the atmospheric environment in urban-forest landscapes. Landscape and Urban Planning, 167, 2017, 348-355.
18. Zgryza Ł., Raczyńska A. and Paśnikowska-Łukaszuk M. Thermovisual measurements of 3D printing of ABS and PLA filaments. Advances in Science and Technology Research Journal, 3(12), 2018, 266–271.